A novel function of Tis11b/BRF1 as a regulator of *Dll4* mRNA 3′-end processing

Agnès Desroches-Castan, Nadia Cherradi, Jean-Jacques Feige, and Delphine Ciais
Institut National de la Santé et de la Recherche Médicale, Unité 1036, Biologie du Cancer et de l'Infection, Grenoble F-38054, France; Commissariat à l'Energie Atomique, Institut de Recherches en Technologies et Sciences pour le Vivant, Grenoble F-38054, France; Université Joseph Fourier-Grenoble 1, Grenoble F-38041, France

ABSTRACT **Tis11b/BRF1 belongs to the tristetraprolin family, the members of which are involved in AU-rich-dependent regulation of mRNA stability/degradation. Mouse inactivation of the *Tis11b* gene has revealed disorganization of the vascular network and up-regulation of the proangiogenic factor VEGF. However, the VEGF deregulation alone cannot explain the phenotype of *Tis11b* knockouts. Therefore we investigated the role of Tis11b in expression of *Dll4*, another angiogenic gene for which haploinsufficiency is lethal. In this paper, we show that *Tis11b* silencing in endothelial cells leads to up-regulation of Dll4 protein and mRNA expressions, indicating that *Dll4* is a physiological target of Tis11b. Tis11b protein binds to endogenous *Dll4* mRNA, and represses mRNA expression without affecting its stability. In the *Dll4* mRNA 3′ untranslated region, we identified one particular AUUUA motif embedded in a weak noncanonical polyadenylation (poly(A)) signal as the major Tis11b-binding site. Moreover, we observed that inhibition of Tis11b expression changes the ratio between mRNAs that are cleaved or read through at the poly(A) signal position, suggesting that Tis11b can interfere with mRNA cleavage and poly(A) efficiency. Last, we report that this Tis11b-mediated mechanism is used by endothelial cells under hypoxia for controlling *Dll4* mRNA levels. This work constitutes the first description of a new function for Tis11b in mammalian cell mRNA 3′-end maturation.**

Monitoring Editor
Marvin P. Wickens
University of Wisconsin

Received: Feb 22, 2011
Revised: Jul 22, 2011
Accepted: Jul 29, 2011

INTRODUCTION

Although underestimated for a long time, posttranscriptional regulation is now recognized as a key control mechanism of gene expression. Splicing, maturation, 3′-end processing, and stability represent major levels of regulation of mRNA levels. Thus RNA-binding proteins (RBPs) involved in the different steps of posttranscriptional regulation are key players in this process (Moore, 2005). Among them are members of the tristetraprolin family, nucleocytoplasmic shuttling proteins that were first characterized as mRNA-destabilizing proteins (Baou *et al.*, 2009). In humans, the tristetraprolin family comprises three members: Tis11b/BRF1 (ZFP36-L1), Tis11d/BRF2 (ZFP36-L2), and the best studied, Tis11/TTP (ZFP36), also named tristetraprolin (TTP). All contain a unique CCCH tandem zinc finger (TZF) domain responsible for mRNA binding through short *cis*-acting sequences called AU-rich elements (AREs) present in the 3′ untranslated region (3′ UTR) of target mRNAs. It has been shown that TTP and Tis11b/BRF1 are able to activate and recruit the mRNA decay machineries onto target transcripts, and thus trigger mRNA degradation (Lykke-Andersen and Wagner, 2005). While in vitro overexpression studies suggest that all three family members have redundant RNA-destabilizing activities, the distinct phenotypes of knockout mice indicate that they might have more specific roles in the control of gene expression.

Indeed, mouse inactivation of *Tis11b* gene shows numerous vascular defects throughout the embryo, indicating the importance of

This article was published online ahead of print in MBoC in Press (http://www.molbiolcell.org/cgi/doi/10.1091/mbc.E11-02-0149) on August 10, 2011.

Address correspondence to: Jean-Jacques Feige (jean-jacques.feige@cea.fr) or Delphine Ciais (delphine.ciais@gmx.fr).

Abbreviations used: 3′ UTR, 3′ untranslated region; ARE, AU-rich elements; ß-Gal, ß-galactosidase; DRB, 5,6-dichloro-1-β-D-ribofuranosylbenzimidazole; DTT, dithiothreitol; EMSA, electrophoretic mobility-shift assay; FBS, fetal bovine serum; HMVECd, dermal human microvascular endothelial cells; HuAEC, human umbilical aortic endothelial cells; IP, immunoprecipitation; PAS, poly(A) signals; PBS, phosphate-buffered saline; poly(A), polyadenylation; pRL, Renilla Luciferase plasmid; PTB, polypyrimidine tract–binding protein; RACE, rapid amplification of cDNA ends; RCC, renal cell carcinoma; RIPA, radioimmunoprecipitation assay; RT-PCR, reverse transcriptase PCR; RT-qrtPCR, reverse transcriptase quantitative real time PCR; siRNA, small interfering RNA; TTP, tristetraprolin; TZF, tandem zinc finger; VEGF, vascular endothelial growth factor; VHL, Von Hippel-Lindau.

the Tis11b protein in angiogenesis, which is the process of blood vessel growth from the preexisting vasculature. These defects were associated with an up-regulation of vascular endothelial growth factor (VEGF) protein (Bell *et al.*, 2006). VEGF is such a fine regulator of angiogenesis that genetic inactivation of a single allele induces important vascular defects and subsequent embryonic lethality (Carmeliet *et al.*, 1996; Ferrara *et al.*, 1996). Thus VEGF expression levels are critical for physiology.

In a previous work, we were the first to show that Tis11b is involved in the regulation of VEGF expression, suggesting a role for Tis11b in angiogenesis (Chinn *et al.*, 2002; Ciais *et al.*, 2004). However, VEGF overexpression in transgenic mice induces embryonic lethality, mainly due to cardiovascular defects with no change in embryonic vessel density or caliber (Miquerol *et al.*, 2000). Thus comparing the phenotype of homozygous *Tis11b*$^{-/-}$ knockout mice with that of VEGF-overexpressing transgenic mice indicated that overexpression of VEGF alone cannot account for the vascular defects observed in *Tis11b* knockouts. It is likely that Tis11b might repress other important genes involved in the control of angiogenesis.

Delta-like-4 (Dll4) is a transmembrane ligand of the Notch receptor family, which is involved in cell fate determination (Kume, 2009). Dll4 is specifically expressed in specialized endothelial cells, called "tip cells," which lead the way for sprouting neo-vessels. Dll4 expression in the tip cell regulates angiogenic branching and density by repressing the ability of neighboring cells to respond to angiogenic stimulation (Williams *et al.*, 2006; Hellstrom *et al.*, 2007; Suchting *et al.*, 2007). *Dll4* haploinsufficiency and overexpression both result in embryonic lethality, strongly suggesting that finely tuned regulation of Dll4 expression is required during angiogenesis. Interestingly, we observed that the phenotypes of both transgenic mice overexpressing Dll4 and *Tis11b* knockout mice show strong similarities, as described in Supplemental Table S1. This suggested to us that Tis11b might also regulate Dll4 expression

In this work, to further decipher the role of Tis11b in angiogenesis, we addressed the possibility that Tis11b controls Dll4 expression. In this paper, we present experimental evidence that Tis11b regulates Dll4 expression in endothelial cells and is involved in hypoxia-mediated regulation of Dll4. In addition, we observed that Tis11b does not control *Dll4* mRNA stability, but modulates 3′ end maturation of the transcript through interaction with an ARE located in the polyadenylation (poly(A)) signal. Our work represents the first description of this novel function of Tis11b in mammalian mRNA 3′ processing.

RESULTS

Dll4 is a direct and physiological target of endogenous Tis11b in endothelial cells

To check for the involvement of Tis11b in Dll4 regulation, we performed a small interfering RNA (siRNA)-based experiment to inhibit endogenous Tis11b expression in primary endothelial cells, and we analyzed Dll4 expression. In Figure 1A, Western blot analysis shows a complete repression of Tis11b protein expression when human umbilical aortic endothelial cells (HuAEC) were transfected with either of two specific Tis11b-targeting siRNAs (T11b1 and T11b2), as compared with a negative control siRNA (CTL). The inhibition of Tis11b is accompanied by a substantial increase in Dll4 protein level (Figure 1A). As Tis11b controls mRNA turnover, we quantified *Dll4* mRNA steady-state levels by reverse transcriptase quantitative real time PCR (RT-qrtPCR) in cells that were silenced for *Tis11b* expression or transfected with siCTL siRNA. As shown in Figure 1B, inhibition of *Tis11b* expression induced a significant two- to threefold increase in the *Dll4* mRNA level in HuAEC cells. To exclude a cell

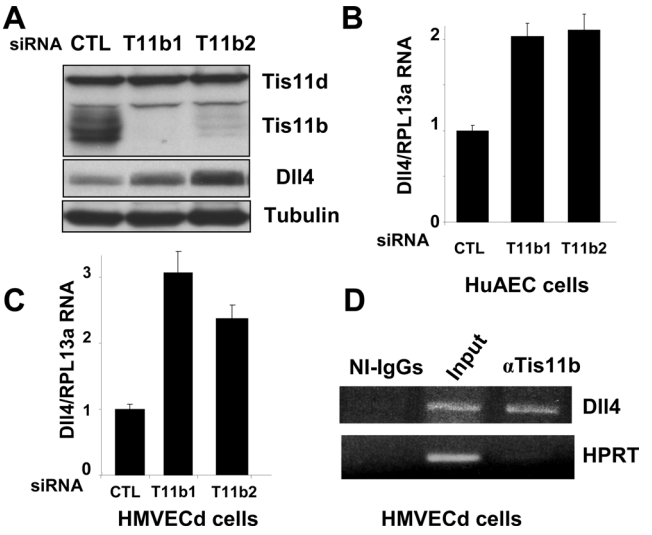

FIGURE 1: Endogenous Tis11b protein targets and regulates *Dll4* mRNA in endothelial cells. (A–C) Inhibition of endogenous Tis11b protein was achieved by transfection of HMVECd or HuAEC with one of the two different siRNAs targeting the human Tis11b sequence (T11b1, T11b2) or negative control siRNA (CTL). (A) Western blot analysis of Tis11b, Dll4, and tubulin in cell extracts from cells depleted of Tis11b protein (T11b1 or T11b2) and control cells (CTL). (B) Steady-state levels of *Dll4* mRNA were quantified by RT-qrtPCR in cell extracts from siTis11b-treated cells (T11b1 or T11b2) or control cells (CTL). (C) Steady-state levels of *Dll4* mRNA were quantified by RT-qPCR in Tis11b-depleted cell extracts (T11b1 or T11b2) or control extracts (CTL). Data are representative of at least three independent experiments. (D) RNP complexes were immunoprecipitated after in vivo cross-linking as described in *Materials and Methods* with anti-Tis11b antibodies (αTis11b) or nonimmune IgG (NI-IgGs). Presence of *Dll4* or *HPRT* mRNA was detected by RT-PCR in the nonprecipitated extracts (Input) or in the immunoprecipitates.

type–dependent effect, the same experiment was performed in dermal human microvascular endothelial cells (HMVECd). As shown in Figure 1C, silencing of *Tis11b* in HMVECd cells also induced an increase in *Dll4* mRNA expression.

To investigate whether Tis11b protein directly interacts with *Dll4* mRNA, we performed RNP (ribonucleoprotein) immunoprecipitation experiments. After cross-linking of endogenous RNP complexes in living cells, we immunoprecipitated Tis11b-containing particles using a specific anti-Tis11b antibody (Ciais *et al.*, 2004; Cherradi *et al.*, 2006) and subjected them to RT-qrtPCR analysis. Figure 1D clearly shows that *Dll4* mRNA was detected in the immunoprecipitated molecular complexes. No *HPRT* mRNA was detected in Tis11b-containing particles, demonstrating that Tis11b protein-*Dll4* mRNA interaction was specific. Moreover, similar data were obtained using a commercial antibody ($\alpha BRF_{1/2}$) that targets a conserved sequence in both Tis11b and Tis11d proteins (unpublished data).

Altogether, these results indicate that *Dll4* mRNA is a direct and physiological target of Tis11b in endothelial cells.

Tis11b does not alter *Dll4* mRNA stability and is mainly localized in the nucleus of endothelial cells

Because Tis11b is known to regulate mRNA stability (Stoecklin *et al.*, 2002), we tested whether Tis11b silencing had an effect on endogenous *Dll4* mRNA turnover rate. Tis11b or CTL siRNAs were transfected in primary endothelial cells, and an inhibitor of RNA polymerase II (5,6-dichloro-1-β-D-ribofuranosylbenzimidazole [DRB])

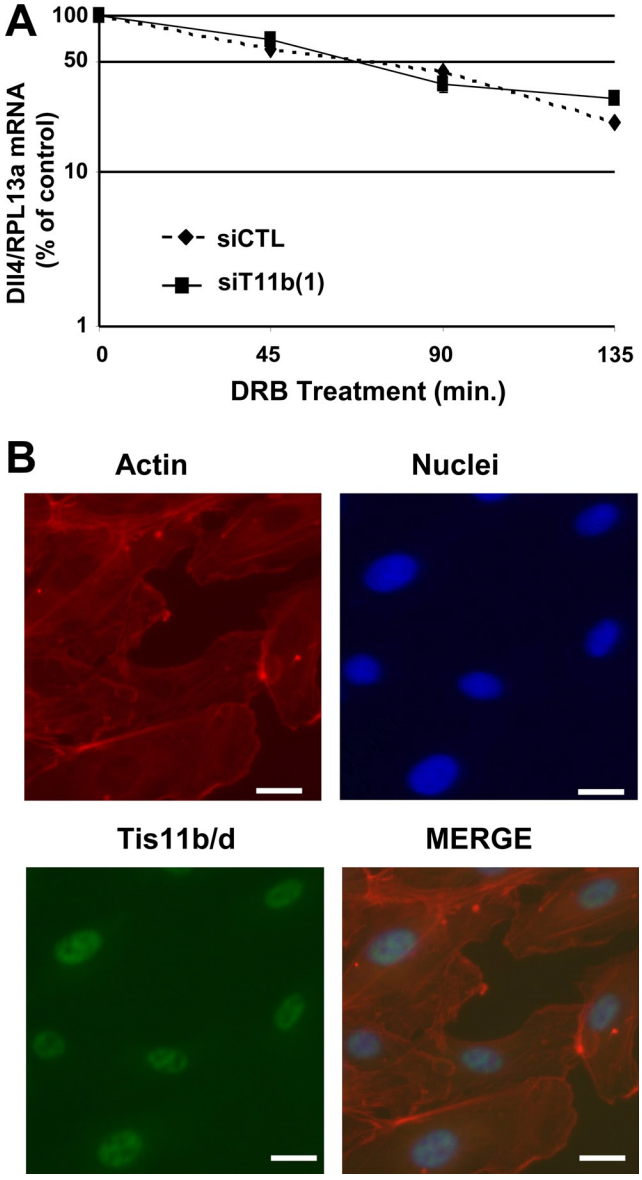

FIGURE 2: Tis11b does not regulate cytoplasmic degradation/stability of *Dll4* mRNA. (A) HuAEC cells were transfected with either an siRNA targeting Tis11b (siT11b1) or an irrelevant siRNA (siCTL). Forty-eight hours after transfection, *Dll4* mRNA decay in the presence of DRB was quantified by RT-qrtPCR analysis. The ratio between *Dll4* mRNA and the housekeeping gene transcript RPL13a levels was normalized at each time point to that measured at time 0 of DRB treatment. Data are representative of five independent experiments. (B) HuAEC cells were stained with phalloidin–Alexa Fluor 555 to visualize actin (red staining), αBRF1 antibodies that detect Tis11b and Tis11d proteins were used to visualize endogenous proteins (green staining), and nuclei were stained with Hoechst 33258 (blue staining). All three stainings were overlaid in the MERGE panel. Data are representative of two independent experiments. Scale bar: 20 μm.

was added 48 h later. We then measured *Dll4* mRNA half-life by RT-qrtPCR. As illustrated in a representative experiment in Figure 2A, no significant difference in *Dll4* mRNA half-life was detected between Tis11b-depleted (siT11b1) and control (siCTL) cells. Quantifications from five independent experiments revealed that the apparent *Dll4* mRNA half-life was 62 ± 12 min in control versus 63.5 ± 25 min in Tis11b-depleted cells.

Control of mRNA stability has been mainly described in the cytoplasm; we therefore analyzed the subcellular localization of endogenous Tis11b in HuAEC by immunofluorescence using an antibody that recognizes both Tis11b and Tis11d ($\alpha BRF_{1/2}$). Figure 2B clearly shows that Tis11b/d immunoreactivity was mainly present in the nucleus. Similar results were obtained in HMVECd (unpublished data).

Altogether, these results suggest that the induction of *Dll4* mRNA observed in Tis11b-depleted endothelial cells is not due to changes in mRNA stability (a process occurring mainly in the cytoplasm), but rather to an unidentified mechanism of regulation of RNA processing that likely occurs in the nucleus.

Identification of potential binding sites for Tis11b protein in *Dll4* mRNA

Tis11b has been shown to bind AREs, which often contain single or multiple copies of the core pentameric AUUUA motif. We therefore checked the human *Dll4* cDNA sequence for consensus AUUUA motifs. We identified one such pentameric motif in close proximity with the cDNA 3′ end. However, we were surprised to observe that this deposited cDNA sequence (NM_019074.2) did not contain a poly(A) tail, and that its poly(A) site was not annotated. We examined the genomic sequences encoding the region around the poly(A) site, which appeared highly conserved between the human, mouse, rat, chicken, and zebrafish species. All contained a second pentameric motif located downstream of the 3′ end of the deposited human Dll4 cDNA sequence. We therefore assumed this cDNA sequence was incomplete. We decided to amplify it by 3′-RACE and to sequence it in order to check whether the second AUUUA motif was actually included in the *Dll4* mRNA. We sequenced 12 amplified clones and identified heterogeneously located poly(A) tail–insertion sites. Five clones revealed an identical poly(A) insertion site defining a "hot spot," whereas in the seven remaining clones, the poly(A) start sites were evenly located on both sides of this hot spot (Figure 3). The analysis of the complete human *Dll4* 3′ UTR cDNA sequences recovered in these experiments allowed us to confirm the presence of the two pentameric AUUUA motifs (named thereafter ARE1 and ARE2) identified in the conserved genomic sequences.

Tis11b regulates Dll4 expression through binding to AU-rich elements in its 3′ UTR

We next tested whether Tis11b exerted its regulation via direct binding to *Dll4* AUUUA motifs. To address this hypothesis, we constructed luciferase reporter plasmids as described in Figure 4A, and transfected them with or without expression plasmids encoding

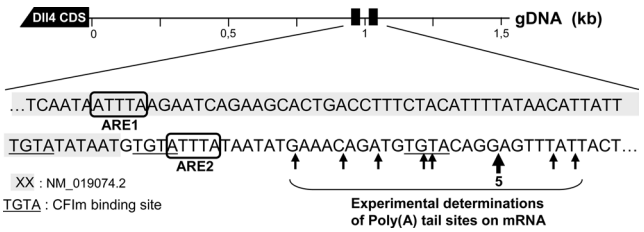

FIGURE 3: Identification of potential binding sites for Tis11b protein in *Dll4* mRNA. 3′-RACE experiments were performed on human endothelial microvascular RNA and 12 clones were sequenced. Sequence in gray background indicates nucleotides present in the NM_019074.2 refseq, boxed sequences are putative binding sites for Tis11b (ARE1 and ARE2), and underlined sequences are UGUA elements. Arrowheads indicate the positions of the added poly(A) tails determined from sequencing and the large arrowhead represents a hot spot found in 5 out of 12 clones.

β-galactosidase (β-Gal) or human Tis11b. We used NIH 3T3 cells for transfection experiments, as these cells express very low levels of Tis11b protein. Transfection of Tis11b protein in these cells had no or little effect on luciferase activity when the *SV40* poly(A) signal was cloned downstream of the luciferase gene (Figure 4B). In contrast, Tis11b expression repressed luciferase expression by ~20–25% when the *SV40* poly(A) signal was replaced by the 2000-nucleotide-long 3′ UTR (Dll4 3′ UTR plasmid). As we located potential binding sites for Tis11b in close proximity to the *Dll4* poly(A) signal, we narrowed down the region of *Dll4*/Tis11b interaction by cloning only the *Dll4* poly(A) signal downstream of the luciferase gene (Dll4pA plasmid). Cotransfection of Tis11b with either Dll4pA or Dll4 3′ UTR plasmid led to a very similar decrease in luciferase expression, indicating that the 125 nucleotides upstream of the poly(A) site are sufficient for Tis11b-mediated control of Dll4 expression. We further analyzed Tis11b interaction with the transcript by introducing mutations in the two pentameric motifs (AUUUA to AGGUA). Individual mutations of either the first AUUUA motif (ARE1) or the second AUUUA motif (ARE2) had no effect on Tis11b ability to reduce luciferase reporter expression. On the contrary, mutations of both motifs (ARE1/2 construction) completely abolished Tis11b-mediated control of luciferase activity. Altogether, these results indicate that the presence of either of the two ARE in this context is sufficient for control of Dll4 expression by Tis11b.

To assess direct binding of Tis11b to the two core pentameric sequences AUUUA, we next performed an electrophoretic mobility-shift assay (EMSA) experiment using recombinant Tis11b protein and radioactive RNA encoding 125 nucleotides upstream of the poly(A) site. As shown in Figure 4C, the addition of recombinant Tis11b induced a shift in the migration of the radiolabeled RNA probe. Moreover, this shift was abolished by the addition of cold competitor, which indicates specific binding of Tis11b protein to *Dll4* mRNA 3′ UTR. In a separate set of in vitro UV cross-linking experiments, we assessed the relative binding between Tis11b protein and Dll4 poly(A) RNA containing mutations on one, two, or none of the AUUUA pentamers. Figure 4D shows that Tis11b protein bound to wild-type RNA and to the ARE1 mutant, but not to the ARE2 mutant or to the ARE1/2 double mutant. These results indicate that ARE2 is the main pentamer responsible for in vitro Tis11b binding onto *Dll4* 3′ UTR.

The efficiency of the weak poly(A) signal of *Dll4* can be modulated by Tis11b

Mammalian poly(A) signals (PAS) are composed of a canonical core A(A/U)UAAA hexamer (or a close variant) located between 10 and 35 nucleotides before a definite site of cleavage and a G/U-rich downstream element (Millevoi and Vagner, 2010). In addition to these signals, and especially in noncanonical PAS, it has been shown that an upstream UGUA element highly contributes to poly(A) signal efficiency via binding of CFIm (Cleavage Factor I), thereby favoring the recruitment of the poly(A) machinery (Nunes *et al.*, 2010). The second AUUUA motif is located 25 nucleotides upstream of the main poly(A) site of *Dll4*, suggesting that the Tis11b-binding site is embedded in the poly(A) signal, which directs the cotranscriptional recruitment of the cleavage/poly(A) machinery (Figure 3). Moreover, it overlaps one of the three UGUA elements present in this poly(A) signal. As we showed that Tis11b is present in the nucleus and that Tis11b can bind to ARE2, we next tested if Tis11b could decrease *Dll4* mRNA by affecting its 3′-end processing in endothelial cells.

To address this question, we constructed a pDll4pA+SV40pA plasmid derived from the previously described pSV40pA and pDll4pA vectors, as illustrated in Figure 5A. pDll4pA+SV40pA

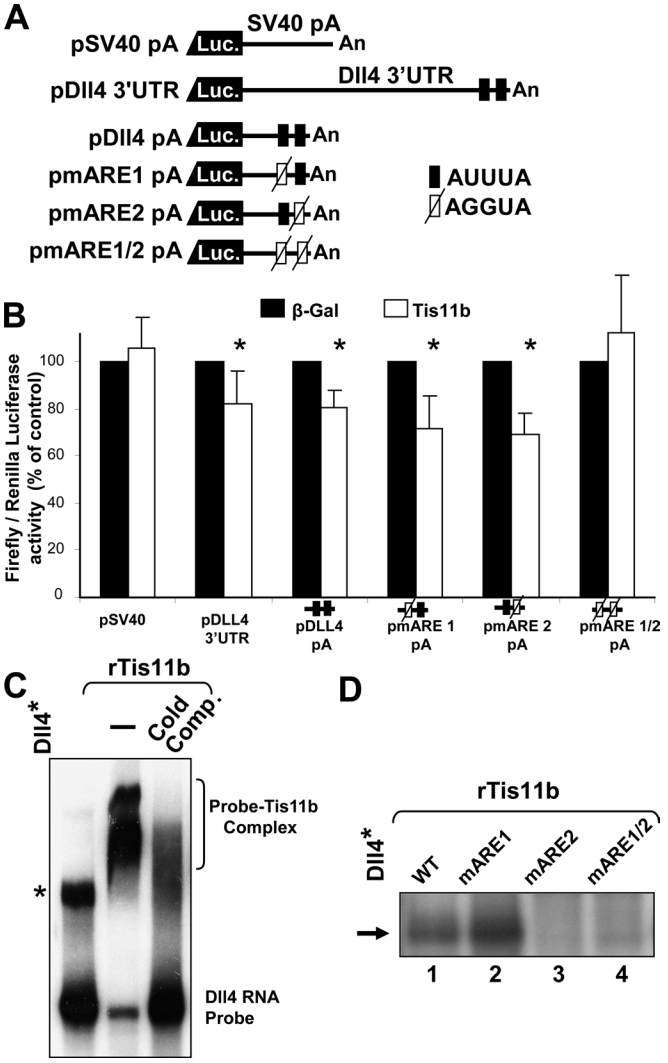

FIGURE 4: Tis11b control of Dll4 expression is AU-rich dependent. (A) Schematic representation of the transfected constructs. The pSV40pA plasmid contains the SV40 PAS cloned downstream of the luciferase gene. For the pDll4 3′ UTR, the 2000 nucleotides downstream of the *Dll4* stop codon were inserted instead of the SV40 PAS of the pSV40pA. For Dll4pA plasmid, the sequence inserted instead of the SV40 PAS begins 125 nucleotides before the expected *Dll4* PAS and extends to the 475 downstream nucleotides. Black rectangles represent the pentameric AUUUA consensus sequences (AREs). Mutations of AREs (mutARE, AUUUA to AGGUA; slashed open rectangles) were introduced in the Dll4pA plasmid. (B) Five nanograms of *Renilla* luciferase-encoding plasmid (pRL) and 250 ng of pDll4 3′ UTR, pDll4pA, pmutARE1, pmutARE2, or pmutARE1+2 plasmids were cotransfected in NIH 3T3 cells with 50 ng of Tis11b- or β-galactosidase-encoding plasmid. Twenty-four hours after transfection, *Renilla* and firefly luciferase activities were measured. Results are expressed as the ratio of firefly to *Renilla* activities normalized to the value observed in the pSV40/ß-Gal condition (taken as 100%). Data are the mean of six independent experiments (*$p < 0.05$). (C) Radiolabeled in vitro transcribed RNA corresponding to the 125 nucleotides upstream of the expected PAS and extending to the 30 downstream nucleotides were incubated with 250 ng of purified Tis11b protein as described in the *Materials and Methods* section in the absence or presence of a 10-fold excess of unlabeled competitor. *, coiled or supercoiled RNA. Data is representative of one experiment. (D) Radiolabeled Dll4 poly(A) RNA with and without mutation of AREs were UV cross-linked to 250 ng of recombinant Tis11b protein and subjected to SDS–PAGE and autoradiography. The arrow points to the position of Dll4-RNA complexes. Data are representative of two experiments.

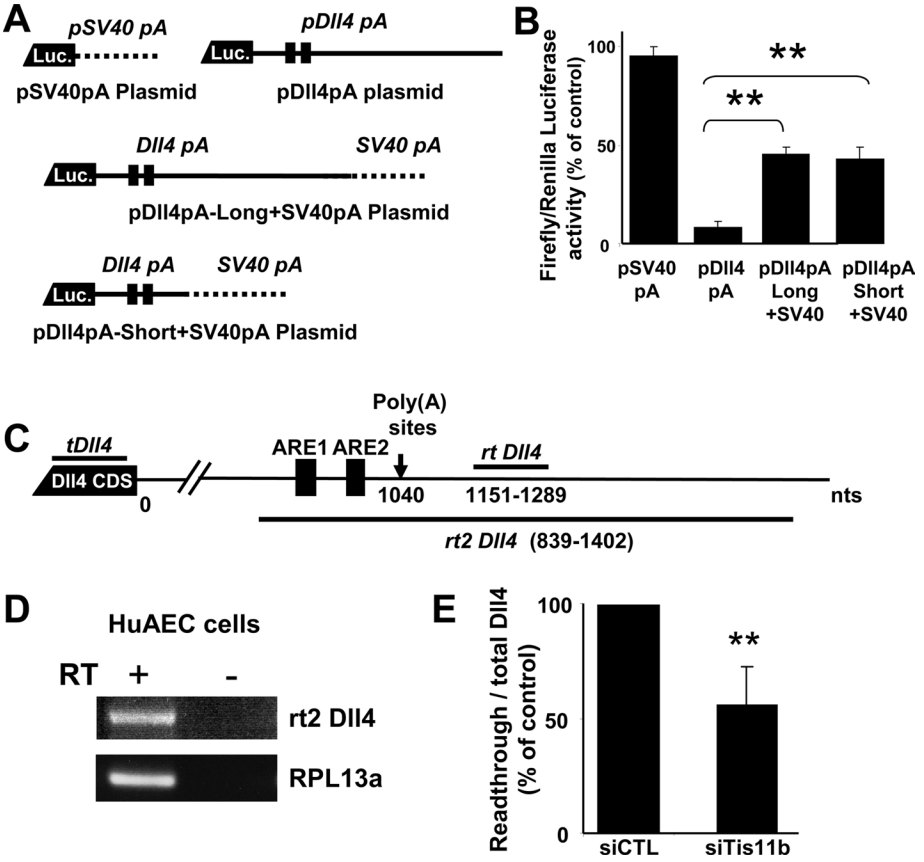

FIGURE 5: Tis11b interferes with cleavage and poly(A) efficiencies. (A) Schematic representation of the plasmids used in NIH 3T3 cell transfections. All plasmids contain the luciferase gene under the control of the thymidine kinase promoter. The pSV40pA plasmid contains the SV40 PAS cloned downstream of the luciferase gene. For Dll4pA plasmid, the sequence inserted in place of the SV40 PAS begins 125 nucleotides before the expected Dll4 PAS and extends to the 475 downstream nucleotides. Plasmids pDll4pA-Long+SV40 and pDll4pA-Short+SV40 are derived from the pDll4pA plasmid with an SV40 PAS added at the end of the Dll4pA sequence or immediately after the Dll4 PAS, respectively. (B) NIH 3T3 cells were cotransfected with 250 ng of pSV40pA, pDll4pA, pDll4pA-Long+SV40pA, or pDll4pA-Short+SV40pA plasmid and 5 ng of pRL for normalization. *Renilla* and *Firefly* luciferase measurements were done 24 h after transfection. Data are the means of six independent experiments (**$p < 0.01$). (C) Representation of the organization of the *Dll4* gene indicating the location of the poly(A) site and the PCR amplifications performed. rtDll4 fragment is encompassing Dll4 poly(A) sites. (D) Total HuAEC RNAs were reverse-transcribed and subjected to RT-PCR detection of the uncleaved Dll4 transcript (rt2Dll4). (E) RT-qrtPCR detection of total Dll4 transcript (tDll4) and readthrough transcript (rtDll4) in Tis11b-depleted HuAEC cells (siT11b) or control cells (siCTL). The ratio of readthrough to total Dll4 transcript levels were normalized to the value measured in siCTL-transfected cells (taken as 100%). Data are the mean of four independent experiments (**$p < 0.01$).

plasmid contains the luciferase reporter gene cloned upstream of the *Dll4* PAS, followed by the *SV40* PAS. Figure 5B shows that pDll4pA luciferase activity is ~10-fold lower than luciferase activity obtained with pSV40pA. On the other hand, insertion of the SV40 PAS downstream of the *Dll4* PAS (pDll4pA-Long+SV40pA plasmid) significantly increased the level of luciferase activity by threefold, indicating that a subpopulation of reporter transcripts is not properly cleaved at *Dll4* PAS. The fact that luciferase activity triggered by pDll4pA-Long+SV40pA plasmid is not completely restored to the level of pDll4pA plasmid suggested that another level of regulation could be mediated by nucleotides downstream of Dll4 poly(A) signal. To assess this, we then shortened the pDll4pA-Long+SV40pA plasmid to make the pDll4pA-short+SV40pA, which contains the SV40 poly(A) signal in close proximity to the *Dll4* PAS (Figure 5A). As shown in Figure 5B, luciferase activities triggered either by pDll4pA-Long+SV40pA or by pDll4pA-short+SV40pA plasmids are similar. Altogether, these results suggest that *Dll4* PAS efficiency is weak and that it might be subjected to subtle regulation.

We next examined whether human *Dll4* PAS is also weak in its genomic context. To this end, we designed reverse and forward primers located on both sides of the *Dll4* PAS for RT-PCR amplification (rt2Dll4), as illustrated in Figure 5C. The 563-nucleotide-long rt2Dll4 amplicon thus encompassed the poly(A) cleavage sites and allowed us to detect the uncleaved transcript. Figure 5D shows detection of the reverse transcriptase (RT)-dependent rtDll4 transcript from HuAEC total RNA. This points out that at least part of *Dll4* mRNA is not fully processed at the poly(A) signal. We further evaluated the possible involvement of Tis11b in cleavage and poly(A) efficiency of *Dll4* PAS. Therefore we quantified total *Dll4* (tDll4) and read-through (rtDll4) transcripts by RT-qPCR analysis in Tis11b-depleted HuAEC cells. Positions of tDll4 and rtDll4 amplicons are shown in Figure 5C. As shown in Figure 5E, inhibition of Tis11b expression decreased the rtDll4/tDll4 ratio by approximately twofold, indicating that the *Dll4* transcript is better processed at poly(A) sites in the absence of Tis11b.

Tis11b participates in the control of *Dll4* mRNA expression under hypoxia

To investigate the contribution of Tis11b in physiological Dll4 regulation, we analyzed Tis11b expression under hypoxic conditions, which are well known to induce Dll4 expression (Patel *et al.*, 2005). Figure 6A shows Western blot analyses of Tis11d, Tis11b, and Dll4 expression in endothelial cells subjected to normoxia or hypoxia (1.5% O_2 for 24 h). As expected, hypoxia induced Dll4 expression in HMVECd or HuAEC. Interestingly, we also could show that the Tis11b protein level was repressed under hypoxic conditions, suggesting a link between hypoxia-controlled Dll4 expression and Tis11b expression levels. As plasmid transfection is very inefficient in primary endothelial cells, we could not test if Tis11b protein overexpression would abrogate hypoxia-increased Dll4 expression. We then performed an RT-qrtPCR analysis of *Dll4* mRNA in endothelial cells depleted or not of Tis11b protein and subjected to normoxia or hypoxia. As shown in Figure 6B, Tis11b depletion or hypoxia induces a clear two- to threefold increase in *Dll4* mRNA, as compared with the normoxic control condition. By contrast, Tis11b depletion under hypoxia results in a weak induction of *Dll4* mRNA (only a 1.3- to 1.5-fold increase). This moderate induction under hypoxia suggests that at least part of the hypoxia-induced regulation of Dll4 is due to Tis11b activity.

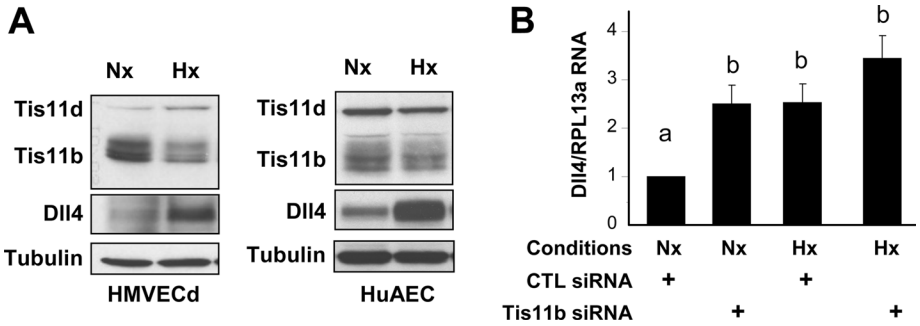

FIGURE 6: Tis11b is involved in hypoxia-mediated Dll4 up-regulation. (A) Western blot analysis of Tis11d, Tis11b, Dll4, and tubulin protein expression in HMVECd and HuAEC cells grown under normoxia (Nx) and hypoxia (Hx, 1.5%O_2). (B) HuAEC cells were cultured under normoxia (Nx) or hypoxia (Hx, 1.5%O_2) for 24 h after siRNA transfection and *Dll4* mRNA transcripts were quantified by RT-qrtPCR analysis. Data are mean of four independent experiments. Values with distinct letters are statistically different ($p < 0.05$).

DISCUSSION

Tis11b is a major modulator of angiogenesis

In this work, we provide evidence that the AU-rich binding protein Tis11b/BRF1 is a direct regulator of *Dll4* mRNA expression in endothelial cells. The identification of Dll4 as a Tis11b target was performed using a siRNA-based strategy to silence Tis11b protein expression. Except for the reporter gene studies used to confirm the AU-rich-dependent effect of Tis11b, we avoided overexpression experiments as much as possible in order to focus on physiological regulation of Dll4 expression. Even though it has been recently described that Tis11b and Tis11d in vivo functions can overlap (Hodson *et al.*, 2010), the Tis11b silencing alone is sufficient to increase *Dll4* mRNA in our study. Although we used two different siRNAs targeting the Tis11d sequence, we were not able to significantly suppress Tis11d protein to address its potential role in Dll4 expression. Moreover, TTP inhibition in endothelial cells had no effect on *Dll4* RNA expression (Supplemental Figure S1), suggesting that physiological control of Dll4 expression by Tis11 family members is restricted to Tis11b.

Interestingly, *Dll4* gene dosage has such a drastic effect on blood vessel development that both genetic haploinsufficiency and overexpression are lethal (Krebs *et al.*, 2004; Trindade *et al.*, 2008). Our work indicates that at least part of the Tis11b$^{-/-}$ phenotype might be due to Dll4 overexpression resulting from Tis11b depletion in endothelial cells. Moreover, we further illustrate Tis11b involvement in angiogenesis by showing that, besides *VEGF*, it regulates the expression of *Dll4*, a second key gene for which haploinsufficiency is known to trigger embryonic lethality.

Among various stimuli inducing VEGF and Dll4 expression, hypoxia plays a major role in inducing tumor angiogenesis and tumor growth. Therefore we examined the hypoxic regulation of Tis11b expression in endothelial cells. We established that hypoxia down-regulates Tis11b expression and that Tis11b is involved in hypoxia-mediated up-regulation of Dll4. This is in contrast with a previous work showing hypoxia up-regulation of Tis11b in human kidney tubular epithelial cells (Sinha *et al.*, 2009). The authors also showed that hypoxia triggered an increase in Tis11b expression in human renal cell carcinoma (RCC), which was reversed by overexpression of the Von Hippel-Lindau (VHL) tumor suppressor gene. Altogether, these observations are in favor of a cell- and context-dependent regulation of Tis11b by hypoxia, which then contributes to modulation of angiogenesis.

Mechanism of Tis11b activity

Both pentameric AUUUA motifs identified in this study contributed to *Dll4* gene control by Tis11b, although no specific interaction between Tis11b protein and ARE1 could be detected in our in vitro binding assay. Nuclear magnetic resonance structure of the Tis11d zinc finger domain (which is very similar to the Tis11b domain) in a complex with the UUAUUUAUU RNA-binding substrate showed that each zinc finger is in contact with a 5′-UAUU-3′ subsite (Hudson *et al.*, 2004). Moreover, according to the AU-Rich Element-Containing mRNA Database (ARED; Bakheet *et al.*, 2006), which clusters human and mouse AU-rich containing transcripts, ARE1 has a sequence of low consensus, with the only core AUUUA. It is possible that Tis11b needs a third partner to stabilize the binding to ARE1 and allow Tis11b-mediated regulation of *Dll4* mRNA.

Tis11b family members are known to be shuttling proteins (Phillips *et al.*, 2002). TTP and Tis11b proteins contain both nuclear localization and export signals and shuttling of the protein is mediated by CRM1-dependent nuclear export. Transfected TTP has been shown to be either nuclear or cytoplasmic, depending on the cell types examined (Johnson *et al.*, 2002; Phillips *et al.*, 2002). In endothelial cells, nuclear sequestration of TTP induced by TNFα treatment abrogates mRNA destabilization, indicating that subcellular localization of the Tis11 family members is part of their mechanism of action (Gringhuis *et al.*, 2005). Here we show that Tis11b is mainly localized in the nucleus of endothelial cells, in contrast with previous reports showing cytoplasmic localization in various cell types (Benjamin *et al.*, 2006; Cherradi *et al.*, 2006). Surprisingly, Tis11b depletion in endothelial cells had no effect on *Dll4* mRNA stability. Taken together, these findings suggest that Tis11b regulates Dll4 expression via a nuclear processing pathway that is independent of *Dll4* mRNA turnover.

It recently has been reported that a yeast homologue of the tristetraprolin family interferes with mRNA 3′-end processing when AU-rich binding sites are located around the poly(A) signal (Prouteau *et al.*, 2008). Interestingly, *Dll4* mRNA PAS contains such a feature, with an efficient AU-rich binding site for Tis11b located less than 30 nucleotides upstream the main poly(A) site (ARE2). Thereby, we speculated that Tis11b binding to *Dll4* pentameric motifs can interfere with 3′-end formation and thus modulate mRNA levels. Indeed, Tis11b depletion in endothelial cells decreases the ratio between Dll4 transcripts stopping at or read through the poly(A) signal, indicating that Tis11b can modulate 3′-end maturation efficiency. It is well known that poly(A) signals contain multiple binding sites for modulators of poly(A) efficiency and that processing of 3′-end maturation can be an important step of regulation (Millevoi and Vagner, 2010). For instance, it has been described that binding of polypyrimidine tract–binding protein (PTB) close to mRNA poly(A) signal could inhibit 3′-end cleavage and poly(A) leading to an increase in readthrough transcripts (Castelo-Branco *et al.*, 2004). Moreover, readthrough transcripts resulting from defective poly(A) are subjected to rapid degradation by the nuclear surveillance pathway which therefore triggers down-regulation of gene expression (Milligan *et al.*, 2005; West and Proudfoot, 2009).

Precise mechanisms of Tis11b modulation of 3′-end maturation remain to be identified. Tis11b binding to *Dll4* AREs might alter the normal recruitment of the cleavage and poly(A) machinery and/or impede the maturation process as schematized in Figure 7. Resulting aberrant transcripts might be detected by the nuclear surveillance pathway, and subsequently degraded by the 3′-exonucleotic

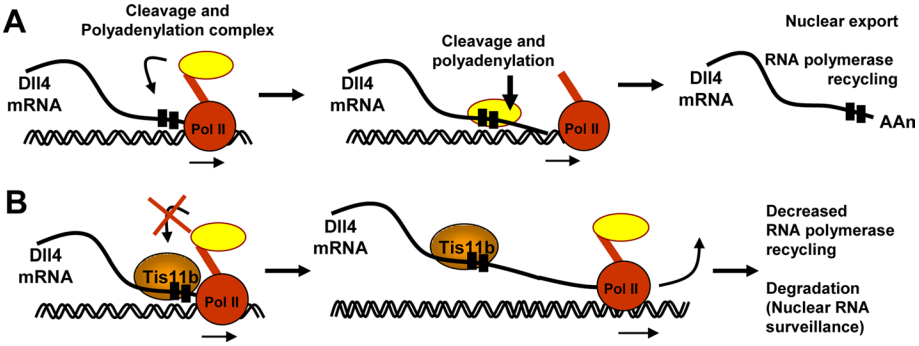

FIGURE 7: Working model of cotranscriptional regulation of *Dll4* mRNA expression by Tis11b/BRF1. (A) Absence of Tis11b at AU-rich sites allows cotranscriptional recruitment of the cleavage and poly(A) machinery, which then performs normal Dll4 3′-end maturation. Mature mRNA is then exported to the cytoplasm. (B) Presence of Tis11b at AU-rich sites impedes or perturbs 3′-end maturation and generates 3′-readthrough transcripts. This defect in 3′-end maturation likely activates nuclear mRNA surveillance and/or attenuates RNA polymerase II recycling, leading to Dll4 expression down-regulation.

activity of the nuclear exosome (Houseley *et al.*, 2006). Moreover, it has been recently described that improper cleavage and poly(A) of mRNA induce defects in RNA polymerase II recycling to the transcription initiation site, leading to down-regulation of gene expression (Mapendano *et al.*, 2010).

To our knowledge, we present here the first evidence of a new function of Tis11b on 3′-end maturation in mammalian cells. These findings might be particularly relevant, considering that more than one-half of human transcripts contain multiple alternative poly(A) sites (Tian *et al.*, 2005). Moreover, most of these poly(A) sites are surrounded by regions with high A and U content that can favor the presence of AREs.

MATERIALS AND METHODS

Cell culture

NIH 3T3 cells were grown in DMEM (Invitrogen, Cergy-Pontoise, France) supplemented with 10% fetal bovine serum (FBS; Invitrogen). Primary endothelial cells (HMVECd and HuAEC) were purchased from LONZA (Basel, Switzerland) and cultivated according to the manufacturer's instructions. All cells were incubated at 37°C in a humid atmosphere in presence of 5% CO_2/95% air atmosphere for normoxic conditions or in 1.5% air atmosphere for hypoxic conditions.

RNA ChIP assay

RNA ChIP assays were performed on HMVECd cells. Tis11b containing ribonucleoprotein complexes was immunoprecipitated with our home-made antibodies, as previously described (Ciais *et al.*, 2004; Cherradi *et al.*, 2006), or with commercial antibodies (#2119; Cell Signaling, Danvers, MA). Ribonucleoprotein complexes were cross-linked by addition of formaldehyde (1% final concentration for 10 min at 37°C), which was then quenched by glycine at 0.125M for 5 min at room temperature. After 2 rinses with phosphate-buffered saline (PBS) containing protease inhibitors (1 mM phenylmethylsulfonyl fluoride, 1 μg/ml aprotinin, 1 μg/ml pepstatin, and 1 μg/ml leupeptin), cells were pelleted by centrifugation for 4 min at 2000 rpm at 4°C. Cells pellets were resuspended in radioimmunoprecipitation assay (RIPA) buffer containing IP. After 30 min on ice, samples were centrifuged 10 min (14,000 rpm, 4°C). Incubation with 20 μl protein A agarose/salmon sperm DNA (50% slurry) for 1 h at 4°C removes nonspecific interactions. After a short centrifugation, the supernatant was immunoprecipitated overnight at 4°C with either antibodies to a peptide fragment (aa 49–63) of Tis11b protein (1:500; CovalAb, Lyon, France) or with $\alpha BRF_{1/2}$ antibodies (#2119; Cell Signaling) at a dilution of 1/250. A negative control was performed with nonimmune rabbit immunoglobulin G (IgG). Antibody–RNA complexes were then collected by addition of 50 μl protein A agarose/salmon sperm DNA (50% slurry) for 1 h at 4°C, and underwent further centrifugation (1500 rpm for 5 min). After four washes with RIPA buffer, elution was done with 100 μl 50 mM Tris-HCl, 5 mM EDTA, 10 mM dithiothreitol (DTT), 1% SDS. Reversion of ribonucleoprotein cross-linking was performed by heating samples at 70°C for 45 min. After centrifugation, the supernatant contained RNA ready for reverse transcription.

siRNA silencing of Tis11b protein in primary endothelial cells

Primary endothelial cells were transfected with siRNA (final concentration: 20 nm/l) targeting human Tis11b sequence using Lipofectamine RNAiMAX from Invitrogen. Two different siRNAs were used to silence Tis11b protein expression to avoid off-target effects, and a nonrelevant siRNA was used to control of specificity. Protein and RNA extractions were done 48 h after siRNAs transfection. All siRNA were purchased from Applied Biosystems (Bedford, MA; #s2089, s2091, and AM4613).

Western blot assay

Two days after siRNA transfection, endothelial cells were lysed in RIPA buffer (10 mM Tris HCl, pH 7.4, 150 mM NaCl, 0.1% SDS, 0.5% Na deoxycholate, 1 mM EDTA, 1% Triton X100, and protease inhibitor cocktail [#P8340; Sigma, St. Louis, MO) for protein extraction. After fractionation of proteins on a 12% SDS–PAGE gel and blotting to a PVDF membrane, immunoblotting detection of Tis11b and Dll4 protein was done using Cell Signaling antibodies according to manufacturer's instructions (#2119 and #2589, respectively). Anti-tubulin antibodies kindly provided by A. Andrieux (Grenoble Institute of Neuroscience, Grenoble, France) were used to check for equal protein loading.

RNA extractions and gene expression analysis by real-time PCR amplification

All RNA extraction was performed using RNAII or RNA XS extraction kits from Macherey-Nagel depending on sample sizes. cDNAs were generated from 1 μg total RNA by reverse transcription using the iScript system (Bio-Rad, Hercules, CA) as recommended by the manufacturer. Real-time PCR was performed using Bio-Rad CFX96 apparatus and qPCR Master Mix (Promega, Charbonnières Les Bains, France). For *Dll4* mRNA half-life measurement, activity of the RNA polymerase II was inhibited by addition of DRB (10 μg/ml) and RNA was extracted at indicated time points. Specific primers used are listed in Supplemental Table S2.

Plasmid constructs

All constructs were cloned into pGL3-basic vector (Promega, Charbonnières Les Bains, France) containing the firefly luciferase gene reporter under the control of a thymidine kinase promoter. 3′ UTR Dll4 and Dll4pA were cloned by PCR on human genomic DNA using primers noted in Supplemental Table S2. The PCR reaction was performed using Advantage GC Genomic LA Polymerase Mix (Clontech, Mountain View, CA). The fragments obtained of 2000 (Dll4 3′

UTR) and 600 (Dll4pA) nucleotides were inserted into pGL3-basic vector between *Xba*I and *Bam*HI sites after removing the SV40 poly(A) signal to create pDll4 3′ UTR and pDll4pA plasmids. Dll4pA-Long pSV40pA and Dll4pA-ShortpSV40pA were obtained by insertion of either a 600-nucleotide-long or a 125-nucleotide-long Dll4pA sequence respectively in pGL3 basic vector *Xba*I site. The pentameric sites were inactivated by transforming the consensus sequence AUUUA to AGGUA on Dll4pA vector. Mutations were performed using overlapping PCR (primers are listed in Supplemental Table S2). All constructs were checked by full-length sequencing (GATC Biotech, Konstanz, Germany).

Tis11b recombinant protein production and purification

The strategy and procedure used to produce recombinant Tis11b has been described elsewhere (Tillet *et al.*, 1997). Briefly, human Tis11b cDNA was inserted in a pCEP4 vector fused with the sequence coding for the signal peptide of human BM40 and with a hemagglutinin tag. Transfection of this plasmid in 293 EBNA cells (Invitrogen) expressing the Epstein Barr Nuclear Antigen 1 allows its episomal replication. Transfected cells are then able to secrete recombinant Tis11b protein in the cell supernatant. Sixty milliliters of this serum-free supernatant was dialyzed three times at 4°C for 4 h against 50 mM sodium phosphate buffer (pH 8.0) containing 300 mM NaCl. The tagged Tis11b protein was purified on nickel-agarose equilibrated in the same buffer and eluted with 250 mM imidazole. The eluate was then dialyzed against 20 volumes of 100 mM Tris/HCl, 100 mM KCl two times for 2 h at 4°C, and determination of protein concentration was performed using the BCA Protein Assay (Pierce, Thermo Fisher, Rockford, IL).

UV cross-linking and EMSA experiments

EMSA and UV cross-linking experiments were performed as previously described (Ciais *et al.*, 2004). Briefly, 5×10^5 cpm of ^{32}P-labeled riboprobes were incubated with 250 ng of recombinant Tis11b protein in 10 mM HEPES (pH 7.6), 3 mM MgCl2, 40 mM KCl, 5% glycerol, 0.5% NP40, and 2 mM DTT. Yeast tRNA (50 ng/ml) and heparin (2 μg/ml) were then added for 10 min. RNA-protein complexes were then resolved by electrophoresis on a native 0.5X TBE-4% acrylamide gel and visualized with a β-Imager. For the UV cross-linking experiment, mixtures were prepared as for EMSA and exposed to UV light for 30 min at 4°C. Then, 100 U of RNase T1 (Invitrogen) was added for 20 min and RNA–protein complexes were analyzed by 10% SDS–PAGE.

Transient transfection and luciferase assay

Subconfluent NIH 3T3 cells were transfected using the Lipofectamine Reagent (Invitrogen). Briefly, for each experiment, 50 ng of plasmid encoding human Tis11b or β-galactosidase was cotransfected with 250 ng of either 3′ UTR Dll4, Dll4pA, mutARE1, mutARE2, or mutARE1+2 plasmid and, for normalization purposes, 5 ng of plasmid encoding *Renilla* luciferase under the control of thymidine kinase promoter (pRL). At 24h posttransfection, measurement of luciferase activities was performed using the Dual-Luciferase Reporter Assay System (Promega, Charbonnières Les Bains, France) according to the manufacturer's instructions. Results are expressed as relative light units of firefly luciferase activity over relative light units of *Renilla* luciferase activity.

Immunofluorescence

HuAEC cells (30,000) were seeded on Lab-Tek chambers (Thermo Fisher Scientific). Cells were fixed using 3% paraformaldehyde in PBS for 15 min at room temperature. After three washes with PBS, cells were permeabilized with 0.5% Triton X-100 for 15 min. Slides were then incubated 1 h at room temperature with rabbit anti-human BRF1/2 antibody (#2119; Cell Signaling) diluted at 1:50. After three rinses, slides were incubated for 1 h at room temperature with cyanine 3-conjugated donkey anti–rabbit IgG (Jackson Immunoresearch Laboratories, West Grove, PA) diluted 1:500 and Phalloidin-Alexa Fluor 555 (A34055; Invitrogen). After washes in PBS, slides were counterstained with Hoechst 33258 (diluted 1:1000) and mounted in Fluorsave (Calbiochem, LaJolla, CA).

3′-end rapid amplification of cDNA ends (3′-RACE)

To determine the localization of the poly(A) site, 3′-RACE was performed as described by (Moucadel *et al.*, 2007). Briefly, 2 μg human endothelial cell RNA was reverse transcribed using Superscript II reverse transcriptase (Invitrogen) in the presence of 500 ng of the $V(T)_{17}$-AP oligo. cDNA was then amplified with a reverse adaptor oligonucleotide (AP) and a forward oligonucleotide (Dll4-F701) located 300 nucleotides upstream of the known end of the human Dll4 3′ UTR. A 23-nucleotide downstream forward oligonucleotide and the same reverse AP primer were used to perform a nested PCR amplification. After gel purification, PCR products were cloned into pCRII-TOPO vector from Invitrogen and 12 clones were sequenced (GATC Biotech). Oligonucleotides are listed in Supplemental Table S2.

Statistical analysis

All results were analyzed by Kruskal-Wallis or Mann-Whitney test. Values of $p < 0.05$ (*) were considered statistically significant.

ACKNOWLEDGMENTS

This work was supported by INSERM (U1036), University Joseph Fourier, CEA (DSV/iRTSV/BCI), and the Association pour la Recherche sur le Cancer (postdoctoral grant to D.C.). We thank A. Andrieux (INSERM U 836, Grenoble Institute of Neuroscience, France), who kindly provided us with anti-tubulin antibodies. We are indebted to S. Bailly (INSERM U 1036, CEA-Grenoble, France) for helpful discussions and suggestions and to E. Tillet (INSERM U 1036, CEA-Grenoble, France) for useful technical advice.

REFERENCES

Bakheet T, Williams BR, Khabar KS (2006). ARED 3.0: the large and diverse AU-rich transcriptome. Nucleic Acids Res 34 (Database issue), D111–D114.

Baou M, Jewell A, Murphy JJ (2009). TIS11 family proteins and their roles in posttranscriptional gene regulation. J Biomed Biotechnol 2009, 634520.

Bell SE, Sanchez MJ, Spasic-Boskovic O, Santalucia T, Gambardella L, Burton GJ, Murphy JJ, Norton JD, Clark AR, Turner M (2006). The RNA binding protein Zfp36l1 is required for normal vascularisation and post-transcriptionally regulates VEGF expression. Dev Dyn 235, 3144–3155.

Benjamin D, Schmidlin M, Min L, Gross B, Moroni C (2006). BRF1 protein turnover and mRNA decay activity are regulated by protein kinase B at the same phosphorylation sites. Mol Cell Biol 26, 9497–9507.

Carmeliet P *et al.* (1996). Abnormal blood vessel development and lethality in embryos lacking a single VEGF allele. Nature 380, 435–439.

Castelo-Branco P, Furger A, Wollerton M, Smith C, Moreira A, Proudfoot N (2004). Polypyrimidine tract binding protein modulates efficiency of polyadenylation. Mol Cell Biol 24, 4174–4183.

Cherradi N, Lejczak C, Desroches-Castan A, Feige JJ (2006). Antagonistic functions of tetradecanoyl phorbol acetate-inducible-sequence 11b and HuR in the hormonal regulation of vascular endothelial growth factor messenger ribonucleic acid stability by adrenocorticotropin. Mol Endocrinol 20, 916–930.

Chinn AM, Ciais D, Bailly S, Chambaz E, LaMarre J, Feige JJ (2002). Identification of two novel ACTH-responsive genes encoding manganese-dependent superoxide dismutase (SOD2) and the zinc finger protein TIS11b [tetradecanoyl phorbol acetate (TPA)-inducible sequence 11b]. Mol Endocrinol 16, 1417–1427.

Ciais D, Cherradi N, Bailly S, Grenier E, Berra E, Pouyssegur J, Lamarre J, Feige JJ (2004). Destabilization of vascular endothelial growth factor mRNA by the zinc-finger protein TIS11b. Oncogene 23, 8673–8680.
Ferrara N, Carver-Moore K, Chen H, Dowd M, Lu L, O'Shea KS, Powell-Braxton L, Hillan KJ, Moore MW (1996). Heterozygous embryonic lethality induced by targeted inactivation of the VEGF gene. Nature 380, 439–442.
Gringhuis SI, Garcia-Vallejo JJ, van Het Hof B, van Dijk W (2005). Convergent actions of I kappa B kinase beta and protein kinase C delta modulate mRNA stability through phosphorylation of 14-3-3 beta complexed with tristetraprolin. Mol Cell Biol 25, 6454–6463.
Hellstrom M, Phng LK, Gerhardt H (2007). VEGF and Notch signaling: the yin and yang of angiogenic sprouting. Cell Adh Migr 1, 133–136.
Hodson DJ *et al.* (2010). Deletion of the RNA-binding proteins ZFP36L1 and ZFP36L2 leads to perturbed thymic development and T lymphoblastic leukemia. Nat Immunol 11, 717–724.
Houseley J, LaCava J, Tollervey D (2006). RNA-quality control by the exosome. Nat Rev Mol Cell Biol 7, 529–539.
Hudson BP, Martinez-Yamout MA, Dyson HJ, Wright PE (2004). Recognition of the mRNA AU-rich element by the zinc finger domain of TIS11d. Nat Struct Mol Biol 11, 257–264.
Johnson BA, Stehn JR, Yaffe MB, Blackwell TK (2002). Cytoplasmic localization of tristetraprolin involves 14-3-3-dependent and -independent mechanisms. J Biol Chem 277, 18029–18036.
Krebs LT, Shutter JR, Tanigaki K, Honjo T, Stark KL, Gridley T (2004). Haploinsufficient lethality and formation of arteriovenous malformations in Notch pathway mutants. Genes Dev 18, 2469–2473.
Kume T (2009). Novel insights into the differential functions of Notch ligands in vascular formation. J Angiogenes Res 1, 8.
Lykke-Andersen J, Wagner E (2005). Recruitment and activation of mRNA decay enzymes by two ARE-mediated decay activation domains in the proteins TTP and BRF-1. Genes Dev 19, 351–361.
Mapendano CK, Lykke-Andersen S, Kjems J, Bertrand E, Jensen TH (2010). Crosstalk between mRNA 3′ end processing and transcription initiation. Mol Cell 40, 410–422.
Millevoi S, Vagner S (2010). Molecular mechanisms of eukaryotic pre-mRNA 3′ end processing regulation. Nucleic Acids Res 38, 2757–2774.
Milligan L, Torchet C, Allmang C, Shipman T, Tollervey D (2005). A nuclear surveillance pathway for mRNAs with defective polyadenylation. Mol Cell Biol 25, 9996–10004.
Miquerol L, Langille BL, Nagy A (2000). Embryonic development is disrupted by modest increases in vascular endothelial growth factor gene expression. Development 127, 3941–3946.
Moore MJ (2005). From birth to death: the complex lives of eukaryotic mRNAs. Science 309, 1514–1518.
Moucadel V, Lopez F, Ara T, Benech P, Gautheret D (2007). Beyond the 3′ end: experimental validation of extended transcript isoforms. Nucleic Acids Res 35, 1947–1957.
Nunes NM, Li W, Tian B, Furger A (2010). A functional human Poly(A) site requires only a potent DSE and an A-rich upstream sequence. EMBO J 29, 1523–1536.
Patel NS, Li JL, Generali D, Poulsom R, Cranston DW, Harris AL (2005). Up-regulation of delta-like 4 ligand in human tumor vasculature and the role of basal expression in endothelial cell function. Cancer Res 65, 8690–8697.
Phillips RS, Ramos SB, Blackshear PJ (2002). Members of the tristetraprolin family of tandem CCCH zinc finger proteins exhibit CRM1-dependent nucleocytoplasmic shuttling. J Biol Chem 277, 11606–11613.
Prouteau M, Daugeron MC, Seraphin B (2008). Regulation of ARE transcript 3′ end processing by the yeast Cth2 mRNA decay factor. EMBO J 27, 2966–2976.
Sinha S, Dutta S, Datta K, Ghosh AK, Mukhopadhyay D (2009). Von Hippel-Lindau gene product modulates TIS11B expression in renal cell carcinoma: impact on vascular endothelial growth factor expression in hypoxia. J Biol Chem 284, 32610–32618.
Stoecklin G, Colombi M, Raineri I, Leuenberger S, Mallaun M, Schmidlin M, Gross B, Lu M, Kitamura T, Moroni C (2002). Functional cloning of BRF1, a regulator of ARE-dependent mRNA turnover. EMBO J 21, 4709–4718.
Suchting S, Freitas C, le Noble F, Benedito R, Breant C, Duarte A, Eichmann A (2007). The Notch ligand Delta-like 4 negatively regulates endothelial tip cell formation and vessel branching. Proc Natl Acad Sci USA 104, 3225–3230.
Tian B, Hu J, Zhang H, Lutz CS (2005). A large-scale analysis of mRNA polyadenylation of human and mouse genes. Nucleic Acids Res 33, 201–212.
Tillet E, Ruggiero F, Nishiyama A, Stallcup WB (1997). The membrane-spanning proteoglycan NG2 binds to collagens V and VI through the central nonglobular domain of its core protein. J Biol Chem 272, 10769–10776.
Trindade A, Kumar SR, Scehnet JS, Lopes-da-Costa L, Becker J, Jiang W, Liu R, Gill PS, Duarte A (2008). Overexpression of delta-like 4 induces arterialization and attenuates vessel formation in developing mouse embryos. Blood 112, 1720–1729.
West S, Proudfoot NJ (2009). Transcriptional termination enhances protein expression in human cells. Mol Cell 33, 354–364.
Williams CK, Li JL, Murga M, Harris AL, Tosato G (2006). Up-regulation of the Notch ligand Delta-like 4 inhibits VEGF-induced endothelial cell function. Blood 107, 931–939.